Variational quantum Monte Carlo calculations for solid surfaces

R. Bahnsen, H. Eckstein, and W. Schattke
Institut für Theoretische Physik und Astrophysik, Christian-Albrechts-Universität Kiel, D-24098 Kiel, Germany

N. Fitzer and R. Redmer
Fachbereich Physik, Universität Rostock, Universitätsplatz 3, D-18051 Rostock, Germany

Quantum Monte Carlo methods have proven to predict atomic and bulk properties of light and nonlight elements with high accuracy. Here we report on variational quantum Monte Carlo (VMC) calculations for solid surfaces. Taking the boundary condition for the simulation from a finite-layer geometry, the Hamiltonian, including a nonlocal pseudopotential, is cast in a layer-resolved form and evaluated with a two-dimensional Ewald summation technique. The exact cancellation of all jellium contributions to the Hamiltonian is ensured. The many-body trial wave function consists of a Slater determinant with parametrized localized orbitals and a Jastrow factor with a common two-body term plus an additional confinement term representing further variational freedom to take into account the existence of the surface. We present results for the ideal (110) surface of gallium arsenide for different system sizes. With the optimized trial wave function, we determine some properties related to a solid surface to illustrate that VMC techniques provide reasonable results under full inclusion of many-body effects at solid surfaces.

PACS number(s): 02.70.Ss, 71.10.-w, 71.15.-m, 73.20-r

I. INTRODUCTION

The theoretical description of solid surfaces bears fundamental aspects as well as technologically important applications. Most of the theoretical approaches are based on density-functional theory (DFT) in the local-density approximation (LDA) or the generalized gradient approximation (GGA). Despite its success a systematic development is hampered by the inherent approximations made, especially for highly correlated or inhomogeneous systems. Therefore, alternative approaches are desirable to test and further develop the quality of the exchange-correlation functional. It is a long tradition to use quantum Monte Carlo (QMC) techniques for the homogeneous electron gas[1] not only to describe the system itself, but also to apply the results as an approximation to inhomogeneous systems. Especially through the use of nonlocal pseudopotentials[2,3] within variational quantum Monte Carlo (VMC), the extension of QMC methods from homogeneous systems to solids of nonlight elements is state of the art with a variety of aspects such as cohesive properties of elemental[4] or bipolar[5,6] solids, or excitation energies.[7–9] For a recent overview we refer the reader to Ref. 10.

Here we propose a scheme to apply the VMC method to solid surfaces. Being safely founded on Ritz's variational principle, all approximations made in the trial wave function are controlled. An unknown functional as in DFT or a perturbative approach like a diagrammatic many-body expansion is thereby avoided. The latter attracted much attention, because of the semiconductor gap problem, through the so-called GW approximation for the self-energy, a termination of the series by setting the vertex function to unity, i. e. $\Sigma = G\,W$.[11,12]

As a model system for semiconductor surfaces the ideal (110) surface of GaAs is chosen. A system with the smallest possible surface unit cell is best suitable for starting practical calculations in order to use the available computational resources to study the finite size behavior along the surface normal. The extension to the reconstructed surface, with a well-established model for the surface geometry available, is straightforward within the presented framework and would offer the chance for quantitative comparison with other theoretical methods and also with experiment. But the huge computational demand makes us restrict ourselves to the ideal surface here.

The paper is organized as follows. In Sec. II, we describe the method with a detailed discussion of the boundary conditions, the Hamiltonian, and the trial wave function. In Sec. III, we present results for the optimization of the confinement term for two different system sizes keeping other surface-specific parameters in the one-body orbitals fixed. The dependence of the total energy on the coordinates of a surface ion is examined to test the sensitivity of the method to surface-specific information.

II. METHOD

A. Stochastic integration

In VMC the expectation value of the Hamiltonian of a quantum system in the state Ψ_λ

$$\langle \hat{H} \rangle = \int \frac{|\Psi_\lambda(\vec{Y})|^2}{\int |\Psi_\lambda(\vec{Y}')|^2 \, d\vec{Y}'} \frac{\hat{H}(\vec{Y})\Psi_\lambda(\vec{Y})}{\Psi_\lambda(\vec{Y})} \, d\vec{Y} \tag{1}$$

is calculated by stochastic integration over the coordinates $\vec{Y}$ of the system, where $\vec{\lambda}$ denotes a set of parameters representing the variational freedom in the trial wave function. In practice the Metropolis algorithm[13] is used to guarantee importance sampling during the random walk so that the energy can be estimated safely as the mean of the local energy with purely statistical error

$$\begin{aligned} \langle \hat{H} \rangle \approx \; E_\lambda &:= \frac{1}{M} \sum_{i=1}^{M} \frac{\hat{H}(\vec{Y}_i)\Psi_\lambda(\vec{Y}_i)}{\Psi_\lambda(\vec{Y}_i)} \, , \\ \sigma(E_\lambda) &= \sqrt{\frac{1}{M} \mathrm{Var}(\frac{\hat{H}\Psi_\lambda}{\Psi_\lambda})} \, . \end{aligned} \tag{2}$$

Ritz's variational principle ensures that the minimum E_{λ^*} of E_λ in the parameter space is an upper bound for the true ground state energy E_0.

B. Boundary conditions for a solid surface

The central problem in a QMC simulation of a solid surface is the choice of the boundary conditions along the surface normal, which is chosen here to be the z axis of the coordinate system. Often a supercell geometry is used to model the semi-infinite crystal: the simulation cell contains a slab of layers surrounded by vacuum on both sides in the z direction, and periodic boundary conditions are applied to all three directions. The use of a localized basis eases the choice of suitable boundary conditions. We assume periodic boundary conditions only in the surface plane and take a symmetric slab of layers with the normalizability of the wave function as the only boundary condition in the z direction. This layer-resolved formulation can be generalized to the semi-infinite crystal as well. The Hamiltonian (see Sec. II C) and the wave function (see Sec. II D) are both affected by the choice of the boundary conditions. First, we describe the adaption of the geometry of the simulation cell to the (110) surface of GaAs.

With the z axis along the [110] direction and the x,y axes in the (110) plane, the following set of vectors spans the lattice of GaAs: $\vec{a}_1 = a\,(1/\sqrt{2}, 0, 0)$, $\vec{a}_2 = a\,(0, 1, 0)$, $\vec{a}_3 = a\,(1/\sqrt{8}, 1/2, 1/\sqrt{8})$, the basis consisting of $\vec{\tau}_{\mathrm{As}} = (0, 0, 0)$ and $\vec{\tau}_{\mathrm{Ga}} = a\,(1/\sqrt{8}, 1/4, 0)$, where a is the lattice constant of cubic GaAs. The two-dimensional lattice $\{\vec{R}^\nu_\parallel\}$ of the simulation cell is chosen as the span of $\vec{b}_1 = N_X \vec{a}_1$, $\vec{b}_2 = N_Y \vec{a}_2$. Denoting the number of lattice planes inside the simulation cell by N_Z, we completely characterize the cell by the triple $(N_X,\, N_Y,\, N_Z)$ containing $N = 8 N_X N_Y N_Z$ electrons and $\mathrm{K} = 2 N_X N_Y N_Z$ ions. N_Z must be large enough to prevent artificial interactions between the two surfaces. Formally the size of the simulation cell in z is infinite because no further assumptions about the z direction are made. That is why no interaction between the two surfaces through the vacuum can occur as in the usual supercell-slab geometry.

To model the infinite solid in this geometry, taking as the third primitive vector $\vec{b}_3 = N_Z (\vec{a}_3)_\perp = N_Z a (0, 0, 1/\sqrt{8})$ gives an orthorhombic simulation cell Ω with the constraint N_Z to be even.

C. Hamiltonian

The Hamiltonian of the considered system, here electrons of a solid or of a solid surface in the Born-Oppenheimer approximation, consists of the kinetic energy operator $\hat{T}$ of the electrons and the potential energy operator $\hat{V}$ of all the Coulomb interactions in the system. For solids of nonlight elements the inner shell electrons and the nucleus can be replaced by a pseudoion with effective charge Z and a nonlocal electron-ion pseudopotential for the valence electrons.[3] The potential energy operator reads

$$\hat{V} = \hat{V}_C + \hat{V}^{\mathrm{l}}_{PP} + \hat{V}^{\mathrm{nl}}_{PP} \;, \tag{3}$$

where $\hat{V}_C$ is the operator of the remaining Coulomb interactions and $\hat{V}^{\mathrm{l}}_{PP}$ and $\hat{V}^{\mathrm{nl}}_{PP}$ are the local and nonlocal part of the pseudopotential, respectively. The nonlocal part is evaluated in a semilocal form.[5] The resulting Coulomb-energy-like operator collects together the constant ion-ion energy, some part of the electron-ion interaction, and the full electron-electron interaction

$$\hat{V}_C = \hat{V}_{ii} + \hat{V}_{ei} + \hat{V}_{ee} \;, \tag{4}$$

thereby including the contributions of the Z/r asymptotic of $\hat{V}^{\mathrm{l}}_{PP}$ among $\hat{V}_{ei}$. The remaining pseudopotential part is short ranged, and only $\hat{V}_C$ is affected by the boundary conditions. To account for the surface-plane-parallel periodic boundary conditions, a super-lattice with the vectors $\{\vec{R}^{\nu}_{\|}\}$ is introduced, which adds to an arbitrary position of charge its periodic counterparts. For clarity and later reference, $\hat{V}_C$ explicitly reads

$$\begin{aligned}
2\hat{V}_C := & \sum_i \left[\sum_{j\neq i} \left(\sum_{\nu} \frac{1}{|\vec{r}_i - \vec{r}_j - \vec{R}^{\nu}_{\|}|} \right) + \sum_{\nu\neq 0} \frac{1}{|\vec{R}^{\nu}_{\|}|} \right] \\
& - \sum_i \sum_{\alpha} \sum_{\nu} \frac{Z_\alpha}{|\vec{r}_i - \vec{R}_\alpha - \vec{R}^{\nu}_{\|}|} \\
& - \sum_{\alpha} \sum_i \sum_{\nu} \frac{Z_\alpha}{|\vec{R}_\alpha - \vec{r}_i - \vec{R}^{\nu}_{\|}|} \\
& + \sum_{\alpha} \left[\sum_{\alpha'\neq\alpha} \left(\sum_{\nu} \frac{Z_\alpha Z_{\alpha'}}{|\vec{R}_\alpha - \vec{R}_{\alpha'} - \vec{R}^{\nu}_{\|}|} \right) + \sum_{\nu\neq 0} \frac{Z_\alpha^2}{|\vec{R}^{\nu}_{\|}|} \right] ,
\end{aligned} \tag{5}$$

where α runs over the index set of gallium and arsenic ions and i over the electrons in the simulation cell. No symmetry between ions in the simulation cell is assumed, so the treatment of reconstructed surfaces is possible without further modifications in the definition of $\hat{V}_C$. As in the three-dimensional case, each of these two-dimensional lattice summations over ν diverges for every $\vec{r}$.

One possibility to overcome this is to introduce a neutralizing background charge in every interaction. To ensure that all these jellium contributions do not artificially change the total Coulomb energy, the background charges are forced to cancel out locally at every point by adding the following terms to $\hat{V}_C$, which vanish due to charge neutrality

$$0 = \left(N - \sum_{\alpha} Z_\alpha \right) \sum_i \sum_{\nu} \frac{1}{\Omega} \int_{\Omega} \frac{-1}{|\vec{r}_i - \vec{R}^{\nu}_{\|} - \vec{R}|} \, d^3R \tag{6}$$

$$0 = \left(-N + \sum_{\alpha'} Z_{\alpha'} \right) \sum_{\alpha} Z_\alpha \sum_{\nu} \frac{1}{\Omega} \int_{\Omega} \frac{-1}{|\vec{R}_\alpha - \vec{R}^{\nu}_{\|} - \vec{R}|} \, d^3R \,, \tag{7}$$

where $\vec{R} = (\vec{R}_{\|}, R_z)$. Splitting up the right-hand side of Eq. (6) into two terms, these are fed into the first and second sum over i of Eq. (5), respectively. In the same way the parts of Eq. (7) are distributed over the sums over α. Now all interactions of Eq. (5) converge and can be calculated separately. We define the following two-dimensional *surface lattice potential* v^s

$$v^s(\vec{r}) := \sum_{\vec{R}^{\nu}_{\|}} \left[\frac{1}{|\vec{r} - \vec{R}^{\nu}_{\|}|} + J^{\nu}(\vec{r}) \right] - \frac{1}{|\vec{r}|} \tag{8}$$

with

$$J^{\nu}(\vec{r}) := \frac{1}{z_0 \Omega^s_0} \int_{-z_0/2}^{+z_0/2} \int_{\Omega^s_0} \frac{-1}{|\vec{r} - \vec{R}^{\nu}_{\|} - \vec{R}|} \, d^2R_{\|} dR_z, \tag{9}$$

where Ω^s_0 is the area of the surface unit cell, and z_0 chosen so that $\Omega = \Omega^s_0 \times [-z_0/2, +z_0/2]$. By generalizing ideas of Ref. 14 we evaluate v^s by Ewald summation technique in the form

$$
\begin{aligned}
v^s(\vec{r}) \;=\; & \sum_{\vec{R}^\nu_\parallel} \left(\frac{1}{|\vec{r}-\vec{R}^\nu_\parallel|} - \frac{1}{|\vec{r}+\alpha\,\mathrm{sgn}(z)\vec{e}_z - \vec{R}^\nu_\parallel|} \right) - \frac{1}{|\vec{r}|} \\
+ \; & \frac{2\pi}{\Omega^s_0} \sum_{\vec{G}_\parallel \neq 0} \frac{\exp[i\,\vec{G}_\parallel \cdot \vec{r}_\parallel - |\vec{G}_\parallel|(|z|+\alpha)]}{|\vec{G}_\parallel|} \\
- \; & \frac{2\pi}{\Omega^s_0} \begin{cases} \alpha, & z \notin [-\frac{z_0}{2}, +\frac{z_0}{2}] \\ \alpha + |z| - \frac{1}{z_0}\left[\left(\frac{z_0}{2}\right)^2 + z^2\right], & z \in [-\frac{z_0}{2}, +\frac{z_0}{2}]. \end{cases}
\end{aligned}
\tag{10}
$$

The result for $\hat{V}_C$ for the simulation of the surface system reads

$$
\begin{aligned}
\hat{V}_C = & \frac{1}{2}\sum_{i,j} [v^s(\vec{r}_{ij})] + \frac{1}{2}\sum_{i\neq j} \frac{1}{|\vec{r}_{ij}|} \qquad (11) \\
& - \sum_{i,\alpha} [Z_\alpha v^s(\vec{r}_{i\alpha})] - \sum_{i,\alpha} \frac{Z_\alpha}{|\vec{r}_{i\alpha}|} \\
& + \frac{1}{2}\sum_{\alpha,\alpha'} [Z_\alpha Z_{\alpha'} v^s(\vec{r}_{\alpha\alpha'})] + \frac{1}{2}\sum_{\alpha\neq\alpha'} \frac{Z_\alpha Z_{\alpha'}}{|\vec{r}_{\alpha\alpha'}|} \\
& + \hat{V}_J(\{z_i\},\{z_\alpha\}) \\
= & \hat{V}_s + \hat{V}_J \,, \qquad (12)
\end{aligned}
$$

where $\vec{r}_{ab} = \vec{r}_a - \vec{r}_b$ and $z_\alpha = (\vec{R}_\alpha)_z$. The Coulomb interaction is decomposed into a term $\hat{V}_s$ depending on the interparticle difference vector only, which gives the main contribution to the total energy, and into a term $\hat{V}_J$, which collects up all remaining terms. As is shown in Appendix A, these depend on z coordinates only. Appendix B contains details of the numerical implementation.

The everywhere bounded, relatively smooth surface lattice potential v^s is used per tabulated interpolation with a Herman-Skilman mesh in z direction. The tabulation is necessary to make practical calculations feasible.

D. Wave function

Our ansatz for the wave function $\Psi = \Psi_S \Psi_J$ consists of a product Ψ_S of Slater determinants and a Jastrow factor Ψ_J with a two-body term and a confinement term

$$
\begin{aligned}
\Psi(\vec{r}_1\sigma_1,\ldots,\vec{r}_N\sigma_N) = & D^\uparrow(\vec{r}_1,\ldots,\vec{r}_{N/2}) D^\downarrow(\vec{r}_{N/2+1},\ldots,\vec{r}_N) \\
& \times \exp\Big[-\sum_{i<j} u(\vec{r}_{ij},\sigma_{ij}) - \sum_i v_{cf}(\vec{r}_i)\Big]
\end{aligned}
\tag{13}
$$

with σ_{ij} denoting parallel or antiparallel spins. The two-body term u is chosen in a periodic form

$$
u(\vec{r},\sigma) = A\Big[\frac{1}{r} + v^s(\vec{r})\Big]\left(1 - e^{-r/F(\sigma)}\right) \ . \tag{14}
$$

A is a variational parameter and $F(\sigma)$ is, for given A, fixed by the cusp condition[15] to compensate for the Coulomb singularity.

The original formulation of Fahy, Wang, and Louie[2,3] included a one-body function $\chi(\vec{r}_i)$ in order to correct for the effect of the two-body term u of smoothing the electron charge density, and to restore the LDA charge density. This idea has been extended successfully to enlarge the variational freedom in the Jastrow factor keeping the one-body states in the Slater determinant unchanged.[4] But one drawback of this approach is that the node surface of Ψ is entirely determined by Ψ_S so that, e.g., further diffusion quantum Monte Carlo calculations are restricted to the quality of the node surface of the underlying VMC wave function that in fact depends on the quality of the one-body orbitals.

Our approach allows for a direct optimization of the one-body orbitals in the Slater determinant,[5] viz.,

$$\begin{aligned}\phi_{\alpha\mu}(\vec{r}) &= \phi^{\mathrm{As}}_{\alpha\mu}(\vec{r}) + \beta\phi^{\mathrm{Ga}}_{\tilde{\alpha}\mu}(\vec{r})\,, \\ \phi^{\mathrm{As}}_{\alpha\mu}(\vec{r}) &= \gamma^{\mathrm{As}}\phi^{\mathrm{As}}_{s}([\vec{r}-\vec{R}^{\mathrm{As}}_{\alpha}]/\zeta^{\mathrm{As}}_{s}) + \sum_i \tau^i_\mu \phi^{\mathrm{As}}_{p_i}([\vec{r}-\vec{R}^{\mathrm{As}}_{\alpha}]/\zeta^{\mathrm{As}}_{p})\,, \\ \phi^{\mathrm{Ga}}_{\tilde{\alpha}\mu}(\vec{r}) &= \gamma^{\mathrm{Ga}}\phi^{\mathrm{Ga}}_{s}([\vec{r}-\vec{R}^{\mathrm{Ga}}_{\tilde{\alpha}}]/\zeta^{\mathrm{Ga}}_{s}) - \sum_i \tau^i_\mu \phi^{\mathrm{Ga}}_{p_i}([\vec{r}-\vec{R}^{\mathrm{Ga}}_{\tilde{\alpha}}]/\zeta^{\mathrm{Ga}}_{p})\end{aligned} \tag{15}$$

for a zinc-blende system as GaAs. The index α here only runs over the set of arsenic ions in the simulation cell, μ over the four tetrahedral directions $\vec{\tau}_\mu$ originating from an arsenic ion, and i over the Cartesian coordinates (x, y, z). The index $\tilde{\alpha}$ denotes the index of the corresponding gallium ion for each bond and is fixed for given α and μ. These localized orbitals are parametrized hybrid bonds with seven variational parameters β, γ, ζ in the bulk case. Especially the contraction parameters ζ allow for compensation of the Jastrow factor. The unmodified orbitals $\phi^{\mathrm{Ga}}, \phi^{\mathrm{As}}$ are $4s$ and $4p$ pseudo wave functions corresponding to the nonlocal *ab initio* LDA, generalized norm-conserving atomic pseudopotential following Hamann.[16,17]

In the construction of the localized one-body orbitals for the arsenic ions in the outermost layer, the corresponding gallium bond partners are missing and new parametrized surface states have to be set.

Our ansatz for the one-body surface states consists of a doubly occupied arsenic dangling-bond orbital. It formally arises from the bulk orbitals of Eq. (15) by setting $\beta = 0$ if α denotes an arsenic ion in the outermost layer and $\mu = \mu_{db}$ denotes a tetrahedral direction towards the vacuum. Apart from $\gamma^{\mathrm{DB}}_p, \zeta^{\mathrm{DB}}_s$, and ζ^{DB}_p as three new surface-specific composition and contraction parameters we allow for the variation of the direction of the dangling-bond orbital by introducing two parameters, the angles ϑ and ϕ, determining the prefactor $\tau^i_{\mu_{db}}$. To allow for effects of relaxation and reconstruction, i.e., the deviation of the ions from their ideal positions, the prefactors τ^i_μ in the construction of the hybrid orbitals are chosen proportional to the vector connecting two neighboring ions. Using localized orbitals as basis functions allows for this automatic adjustment to deviations from the ideal lattice. That might not be sufficient for an arbitrarily complex surface rearrangement, however, in many cases of real surfaces it probably will be flexible enough.

With this variational freedom one would expect that on increasing the number of layers the total energy per atom comes asymptotically closer to the theoretical bulk value because the surface to bulk fraction decreases. But, as will be stated in Sec. III B, the energy actually increases instead of decreasing with increasing system size. To compensate for the observed overshoot in smoothing the electron density over the whole range of the simulation cell by the Jastrow factor, we introduce the following confinement term in the Jastrow factor

$$v_{cf}(\vec{r}) \equiv v_{cf}(z) = \frac{1}{2} V_{cf}\left[\tanh\{S_{cf}(|z| - z_{cf} - L_{cf})\} + 1\right], \tag{16}$$

where z_{cf} is the z distance of the outermost layer from the center.

Altogether eight surface-specific parameters are introduced, five for the single-particle orbitals and three for the confinement term.

III. RESULTS AND DISCUSSION

A. Bulk

In order to test the numerical implementation of the layer-resolved formulation of the Hamiltonian, of the geometry of the simulation cell, and of the construction of the trial wave function by comparison with independently obtained results, a bulk GaAs system is modeled by an orthorhombic cell called (2,2,8) containing 256 electrons. Usual three-dimensional boundary conditions are applied for the random walk, but two-dimensional boundary conditions are applied for the Coulomb potential and a direct summation is carried out over the copies in z direction, which can be truncated after a small number of copies because the potential is vanishing rapidly with increasing z distance. The total energy is determined for different cubic lattice constants a keeping all other variational bulk parameters fixed. The resulting minimal energy per unit cell $E^b = (-232.92 \pm 0.05)$ eV/u.c. at an equilibrium lattice constant of $a^b_0 = (10.69 \pm 0.05)$ a.u. is in very good agreement with our former results of $E^{\mathrm{ref}} = (-233.04 \pm 0.08)$ eV/u.c. at an equilibrium lattice constant of $a^{\mathrm{ref}}_0 = (10.69 \pm 0.1)$ a.u. obtained within the usual VMC scheme for solids for the same number of electrons.[5]

We conclude from this comparison that, with respect to numerical accuracy, the layer-resolved implementation is suitable to tackle the many-body problem for solid surfaces.

B. Solid surface

First, VMC calculations without confinement terms were performed. All calculations were carried out with our highly parallelized QIRM package.[18] Typical lengths of simulation runs are 2000 steps per electron for equilibration and integration each, taking approximately 4 and 10 hours on an ALPHA EV56 CPU for 256 and 384 electrons, respectively. In principle, a full optimization over the eight-dimensional parameter space has to be carried out. Optimization in high-dimensional space in the presence of noise is a business of its own. To reduce the huge computational effort and to learn about the influence of the parameters, a step by step optimization of the most significant parameters is adequate here.

Only technically necessary changes due to the new form of the simulation cell, due to the prescribed two-dimensional periodicity concerning the Hamiltonian, the trial wave function, and the random walk, and due to the lack of binding partners for ions at the outermost layers were made. One would expect that with increasing number of layers the energy should converge to the asymptotic of the (theoretical) bulk energy E^b. But for the surface system (2,2,8) an energy of $E^s = (-154.13 \pm 0.16)$ eV/u.c. is obtained. What is even worse, increasing the number of layers up to 12, the total energy increases monotonically with an average slope of 24 eV/layer. So a straightforward, brute-force usage of the traditional VMC scheme does not seem possible. Experience with bulk results shows that finite-size effects are of the order of eV.[19] We suppose that this is similar in surface-parallel direction and therefore do not consider them here.

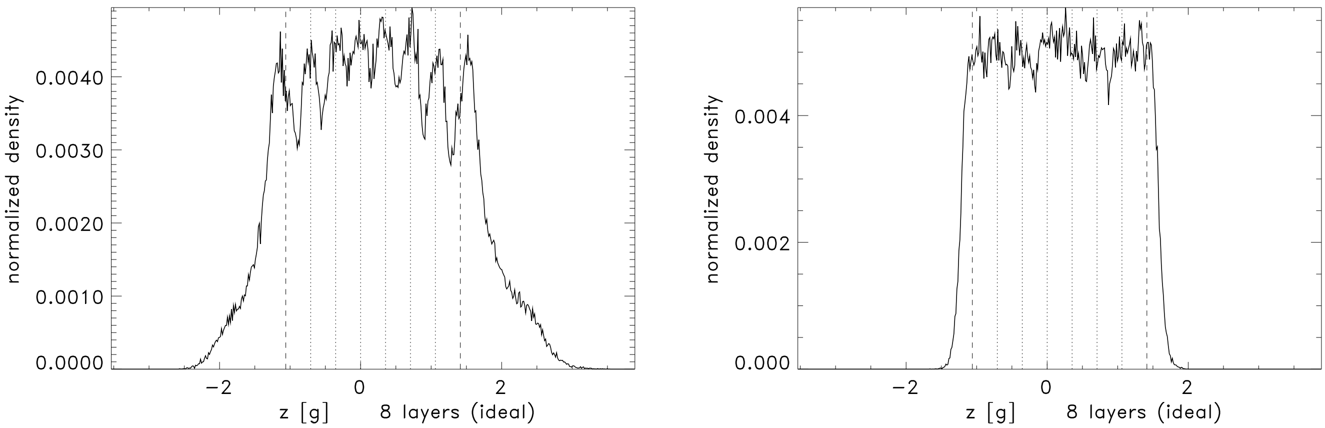

FIG. 1. z-resolved density with (right) and without (left) confinement term in the trial wave function

Analyzing the different contributions to the total energy, one finds that with respect to the bulk case, a per unit cell decrease in the positive electron-electron interaction for larger systems is drastically overcompensated by an increase in the negative electron-ion interaction. This trend is even sharpened for bigger system sizes. Such drastic changes seem to be caused by electrons drifting extraordinarily far into the vacuum region. The actual existence of this mechanism is proved by observation of the z-resolved density. As one can see from the left part of Fig. 1 the electron density is smeared out into the vacuum regions. This behavior comes from the known effect of the two-body part of the Jastrow factor of smoothing the electron density. In the bulk case, we have compensated for this effect through the introduction of contraction parameters in the localized orbitals of the Slater determinant. But here, having allowed the outermost, arsenic dangling-bond orbitals to be contracted, we find no significant improvement on the relevant scale of 10 eV.

Taking advantage of the flexibility of VMC as a variational procedure, we introduce an additional factor in the trial wave function allowing for a compensation of the Jastrow pressure on the scale of the whole surface system. Formally, this factor belongs to the Jastrow term in the form of a z-dependent confinement function v_{cf}.

To examine the behavior of the total energy with respect to the variation of the three confinement parameters, calculations for the system (2,2,8) with 256 electrons were performed yielding a minimal energy of $E^s_{256} = (-223.00 \pm 0.99)$ eV/u.c. for $(V_{cf}, S_{cf}, L_{cf}) = (15.15 \pm 1.64, 0.137 \pm 0.013, 3.01 \pm 0.77)$. This is an essential improvement in comparison to the former results. The optimization was done by a weighted regression where the total energy is written as a quadratic function of the variational parameters.

In the region of parameter space where the global minimum is actually located, the information of one of the three parameters is redundant due to the presence of noise in the form of the statistical uncertainty of the Monte Carlo data E_λ. It is sufficient to fix one parameter at an approximately correct value. E.g., setting $L_{cf} = 3.0$ a.u. and scanning the remaining two-dimensional parameter space yields a fitted energy of $\tilde{E}^s_{256} = (-222.92 \pm 2.16)$ eV/u.c. for $(V_{cf}, S_{cf}, L_{cf}) = (15.27 \pm 0.24, 0.139 \pm 0.006, 3.0)$. Finally, gathering statistics yields $\bar{E}^s_{256} = (-222.86 \pm 0.05)$ eV/u.c. We conclude that the actual uncertainty in energy is of the order of 100 meV/u.c. and that the trial wave function is essentially improved. Computed with the optimized trial wave function, now the z-resolved density as seen in the right part of Fig. 1 is much more localized to the solid proving that the above reasoning to explain the failure of the bulk derived trial wave function was correct.

If the new confinement term is generally suitable also for larger systems, the trend of increasing energy with number of layers should be reversed. Therefore we performed calculations for the system (2,2,12) with 12 layers and 384 electrons. Again a two-dimensional scan of the total energy landscape was performed yielding a fitted optimal energy of $\tilde{E}^s_{384} = (-223.64 \pm 2.09)$ eV/u.c. for $(V_{cf}, S_{cf}, L_{cf}) = (32.68 \pm 0.21, 0.103 \pm 0.001, 3.0)$. Repeated sampling with these values of parameters gives $\bar{E}^s_{384} = (-223.52 \pm 0.06)$ eV/u.c.

So by increasing the system size a slight decrease in total energy is found that was originally to be expected from physical reasoning. Comparing the optimal values for the variational parameters underlines that the bigger system needs a higher compensation of the Jastrow pressure that is reflected in the corresponding values of V_{cf} and S_{cf}.

To get a realistic total energy, now on the scale of 1 eV, further lowering has to be achieved by other variational degrees of freedom, e.g., by variation of parameters in the one-body orbitals in the Slater determinant. These results will be presented in a forthcoming publication.

Here in the rest of this section we focus on the question that to which extent the proposed VMC procedure can resolve surface-specific information. As a test case an in-layer displacement of the arsenic ions in the outermost layer is chosen. Is this statistically resolvable within the current stage of optimization of the trial wave function? To improve the flexibility of the trial wave function with respect to ion displacement, the coefficients of the p_i orbitals are chosen so that the resulting hybrid bond orbitals are automatically concentrated in the bond direction keeping all other variational surface-specific parameters fixed. In Fig. 2 the total energy per unit cell is plotted against the displacement of an arsenic ion perpendicular to the As-Ga chains of the ideal (110) surface. Despite the presence of statistical noise a minimum is clearly detectable. The equilibrium position is found very close to the ideal position slightly moved to the direction away from the As-Ga chains. So the determination of elements of the dynamical matrix via a parabolic fit is statistically relevant within this VMC procedure.

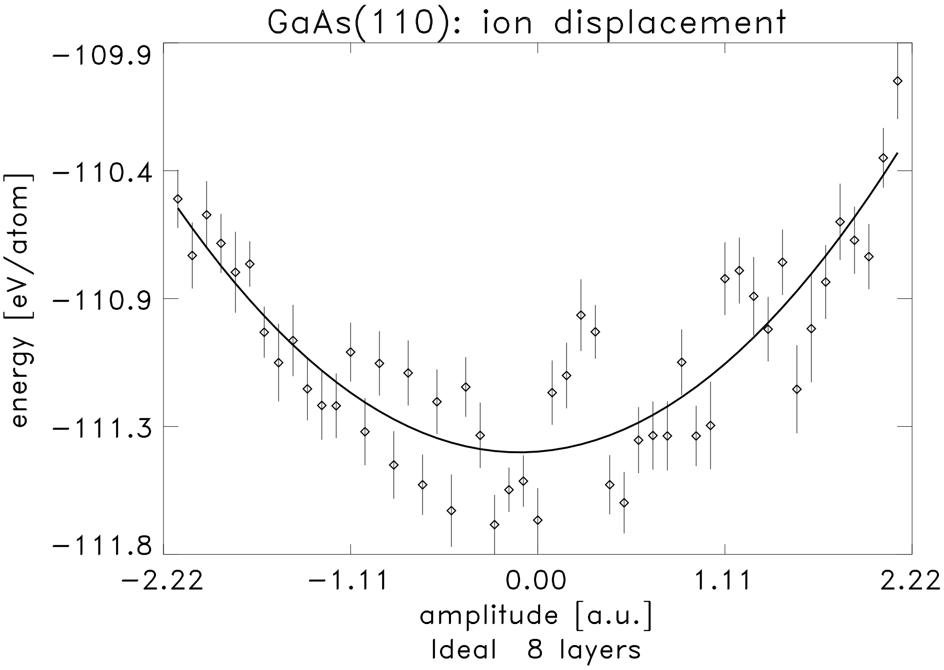

FIG. 2. Total energy in [eV/atom] of slab of 8 layers with outermost arsenic ions displaced within layer plotted against displacement in atomic units. Error bars denote the statistical uncertainty $\sigma(E_\lambda)$ of individual Monte-Carlo energies E_λ. Solid line shows the best fitting parabola.

In conclusion, we proposed a scheme to describe solid surfaces in the frame of VMC techniques in order to use their fundamental aspects also in this field. An Ewald technique has been introduced for two-dimensional systems, which uses an exact compensation of background charges. Starting from a bulk derived, only slightly modified trial wave function showed a failure with respect to finite-size analysis. The reason was found in a large drift of the electron density into the vacuum. By introducing a confinement term to the trial wave function, much better results, with respect to the absolute value in total energy and with respect to the size dependence, were obtained.

Future work should focus on the automatic adjustment of the trial wave function to relaxation of the ions in order to introduce as few variational parameters as possible, and on the global optimization in the presence of noise. Then a comparison of ideal and reconstructed surface models will become tractable.

The sensitivity and relevance of the technique to surface structures could be proved showing that a surface analysis is feasible. This should allow a start from a well-founded, variational basis to finally yield surface-specific statements like relaxation or reconstruction, and many-body influences therein.

ACKNOWLEDGMENTS

We thank D. Lukas and D. Schulz for valuable discussions. Support from the Deutsche Forschungsgemeinschaft under Grants No. Scha 360/8-1 and No. Scha 360/17-1 is gratefully acknowledged. The calculations were performed on the CRAY-T3E at the Konrad-Zuse-Zentrum für Informationstechnik, Berlin.

APPENDIX A: EXPLICIT FORM OF V_J

After insertion of Eqs. (6) and (7) into Eq. (5) and regrouping, four terms like

$$\begin{aligned}2V_{ab} &= \sum_{\gamma}^{N_a}\sum_{\gamma'\neq\gamma}^{N_b}\sum_{\nu}\left(\frac{1}{|\vec r_\gamma-\vec r_{\gamma'}-\vec R_\parallel^\nu|}+\frac{1}{\Omega}\int_\Omega\frac{-1}{|\vec r_\gamma-\vec R_\parallel^\nu-\vec R|}\,d^3R\right) &\text{(A1)}\\ &+\sum_{\gamma}^{N_a}\left[\sum_{\nu\neq0}\left(\frac{1}{|\vec R_\parallel^\nu|}+\frac{1}{\Omega}\int_\Omega\frac{-1}{|\vec r_\gamma-\vec R_\parallel^\nu-\vec R|}\,d^3R\right)+\int_\Omega\frac{-1}{|\vec r_\gamma-\vec R|}\,d^3R\right]\\ &=:\sum_\gamma\sum_{\gamma'}\sum_\nu{}'\left(\frac{1}{|\vec r_\gamma-\vec r_{\gamma'}-\vec R_\parallel^\nu|}+\frac{1}{\Omega}\int_\Omega\frac{-1}{|\vec r_\gamma-\vec R_\parallel^\nu-\vec R|}\,d^3R\right) &\text{(A2)}\end{aligned}$$

occur, where γ can either run through an electron index set or an ion index set, read $\gamma=\alpha$ or $\gamma=i$ in Eq. (5), respectively. The prime at the summation over ν means that the divergent term $1/|\vec R_\parallel^{\nu=0}|$ has to be skipped in the $\nu=0$ term of the sum if the outer indices γ and γ' are equal and denote the same particle, however, with the associated integral still being kept.

Substituting $\vec R' := \vec R_\parallel^\nu + \vec R$ and skipping the prime, the volume of integration changes from $\Omega=\Omega_0^s\times[-z_0/2\,,+z_0/2]$ to $\Omega_\nu := \Omega+\vec R_\parallel^\nu =: \Omega_\nu^s\times[-z_0/2\,,+z_0/2]$. Defining $\Omega_\infty := (\sum_\nu\Omega_\nu^s)\times[-z_0/2\,,+z_0/2]$ Eq. (A2) now reads

$$2V_{ab}=\sum_\gamma\sum_{\gamma'}\left[\sum_\nu{}'\left(\frac{1}{|\vec r_\gamma-\vec r_{\gamma'}-\vec R_\parallel^\nu|}\right)+\frac{1}{\Omega}\int_{\Omega_\infty}\frac{-1}{|\vec r_\gamma-\vec R|}\,d^3R\right]\,. \quad \text{(A3)}$$

The next step is to substitute $\vec R=\vec R'+\vec r_{\gamma'}$ in the integrals and skipping the prime again. Now the integration runs over $\Omega_\infty^{\gamma'} := (\sum_\nu\Omega_\nu^s)\times[-z_0/2-z_{\gamma'}\,,+z_0/2-z_{\gamma'}]$. Furthermore, using the additivity of integration yields

$$\begin{aligned}2V_{ab}&=\sum_\gamma\sum_{\gamma'}\left[\sum_\nu{}'\left(\frac{1}{|\vec r_\gamma-\vec r_{\gamma'}-\vec R_\parallel^\nu|}\right)+\frac{1}{\Omega}\int_{\Omega_\infty}\frac{-1}{|\vec r_\gamma-\vec r_{\gamma'}-\vec R|}\,d^3R\right] &\text{(A4)}\\ &+\sum_\gamma\sum_{\gamma'}[\frac{1}{\Omega}\int_{\Omega_\infty^{\gamma'}-\Omega_\infty}\frac{-1}{|\vec r_\gamma-\vec r_{\gamma'}-\vec R|}\,d^3R]\,.\end{aligned}$$

Integration over $\Omega_\infty^{\gamma'} - \Omega_\infty$ means that contributions from $\Omega_\infty^{\gamma'}$ count positively while Ω_∞ contributes negatively. The first line of Eq. (A4) depends only on the difference vector $\vec{r}_{\gamma\gamma'} := \vec{r}_\gamma - \vec{r}_{\gamma'}$. So it is useful to define

$$v^s(\vec{r}_{\gamma\gamma'}) := \sum_\nu \left(\frac{1}{|\vec{r}_\gamma - \vec{r}_{\gamma'} - \vec{R}_\parallel^\nu|} + \frac{1}{\Omega} \int_\Omega \frac{-1}{|\vec{r}_\gamma - \vec{r}_{\gamma'} - \vec{R}_\parallel^\nu - \vec{R}|} \, d^3R \right) - \frac{1}{|\vec{r}_{\gamma\gamma'}|} \tag{A5}$$

and

$$\varphi^J(z_\gamma, z_{\gamma'}) := \frac{1}{\Omega} \int_{\Omega_\infty^{\gamma'} - \Omega_\infty} \frac{-1}{|\vec{r}_\gamma - \vec{r}_{\gamma'} - \vec{R}|} \, d^3R \, . \tag{A6}$$

Though $\vec{r}_\gamma$ and $\vec{r}_{\gamma'}$ formally appear on the right-hand side of Eq. (A6), the actual dependence on $\vec{r}_\parallel$ drops out due to the infinite integration parallel to the surface. Changing the variable of integration to $\vec{R}' = \vec{R} + \vec{r}_{\gamma'}$ in Eq. (A6) leads to the result

$$\varphi^J(z_\gamma, z_{\gamma'}) = \frac{1}{\Omega} \int_{\Omega_\infty - \tilde{\Omega}_\infty^{\gamma'}} \frac{-1}{|\vec{r}_\gamma - \vec{R}|} \, d^3R \, , \tag{A7}$$

with $\tilde{\Omega}_\infty^{\gamma'} := (\sum_\nu \Omega_\nu^s) \times [-z_0/2 + z_{\gamma'} \, , \, +z_0/2 + z_{\gamma'}]$. Physically this corresponds to a dipole-like charge configuration with films of finite width. A compact solution of this problem of electrostatics is given in Appendix B. Finally, inserting Eqs. (A5) and (A7) in Eq. (A4) with additional prefactors $Z_\gamma, Z_{\gamma'}$ to account for arbitrarily charged particles in the general case, $2V_{ab}$ can be expressed as

$$\begin{aligned} 2V_{ab} &= \left(\sum_\gamma \sum_{\gamma'} Z_\gamma Z_{\gamma'} v^s(\vec{r}_{\gamma\gamma'}) + \sum_\gamma \sum_{\gamma' \neq \gamma} Z_\gamma Z_{\gamma'} \frac{1}{|\vec{r}_{\gamma\gamma'}|} \right) + \sum_\gamma \sum_{\gamma'} Z_\gamma Z_{\gamma'} \varphi^J(z_\gamma, z_{\gamma'}) && \text{(A8)} \\ &=: 2V_{ab}^s + 2V_{ab}^J \, . && \text{(A9)} \end{aligned}$$

With these abbreviations the total Coulomb energy of Eq. (5) can be written as

$$\begin{aligned} V_C &= V_{ee}^s + V_{ee}^J + V_{ei}^s + V_{ei}^J + V_{ie}^s + V_{ie}^J + V_{ii}^s + V_{ii}^J && \text{(A10)} \\ &= V_{ee}^s + 2V_{ei}^s + V_{ii}^s + V_{ee}^J + V_{ei}^J + V_{ie}^J + V_{ii}^J && \text{(A11)} \\ &=: V_s + V_J \, . && \text{(A12)} \end{aligned}$$

APPENDIX B: NUMERICAL EVALUATION OF V_J

As defined in Eq. (A9) $2V_J$ consists of terms like

$$2V_{ab}^J = \sum_{\gamma_a \gamma_b} Z_{\gamma_a} Z_{\gamma_b} \varphi^J(z_{\gamma_a}, z_{\gamma_b}) \, . \tag{B1}$$

Due to the symmetry of the problem φ^J can be expressed by

$$\varphi^J(z_{\gamma_a}, z_{\gamma_b}) = \begin{cases} \varphi_+^J(z_{\gamma_a}; z_{\gamma_b}), & z_{\gamma_b} \geq 0 \\ \varphi_+^J(z_{\gamma_a} - z_{\gamma_b}; z_{\gamma_b}), & z_{\gamma_b} < 0 \, . \end{cases} \tag{B2}$$

Before giving the explicit expression for φ_+^J we define

$$\begin{aligned} d_\rho(|z'|) &= \min(|z'|, z_0) \, , && \text{(B3)} \\ d_0(|z'|) &= \big| \, |z'| - z_0 \, \big| \, . && \text{(B4)} \end{aligned}$$

Then the potential generated by a dipole-like charge distribution of two oppositely charged films each of thickness d_ρ with their inner borders separated by d_0 is given by

$$\varphi_+^J(z;z') = \varphi_0 + \frac{\mathrm{sgn}(z')}{\Omega_0^s z_0} \begin{cases} 0, & z \in (-\infty\,,\, -\frac{z_0}{2}] \\ \frac{1}{2}(z+\frac{z_0}{2})^2, & z \in (-\frac{z_0}{2}\,,\, -\frac{z_0}{2}+d_\rho] \\ d_\rho(z+\frac{z_0}{2}-\frac{d_\rho}{2}), & z \in (-\frac{z_0}{2}+d_\rho\,,\, -\frac{z_0}{2}+d_\rho+d_0] \\ -\frac{z^2}{2}+(-\frac{z_0}{2}+2d_\rho+d_0)(z+\frac{z_0}{2})+ & \\ \frac{1}{2}(\frac{z_0}{2})^2 - d_\rho(d_\rho+d_0) - \frac{d_0^2}{2}, & z \in (-\frac{z_0}{2}+d_\rho+d_0\,,\, -\frac{z_0}{2}+2d_\rho+d_0] \\ d_\rho d_0 + d_\rho^2, & z \in (-\frac{z_0}{2}+2d_\rho+d_0\,,\, +\infty)\,. \end{cases} \tag{B5}$$

The potential is determined up to a constant φ_0. This is fixed by the convention that a charge at $z = -\infty$ feels zero potential leading to $\varphi_0 = 0$.

---

[1] D. M. Ceperley and B. J. Alder, Phys. Rev. Lett. **45**, 566 (1980).
[2] S. Fahy, X. W. Wang, and S. G. Louie, Phys. Rev. Lett. **61**, 1631 (1988).
[3] S. Fahy, X. W. Wang, and S. G. Louie, Phys. Rev. B **42**, 3503 (1990).
[4] A. J. Williamson, S. D. Kenny, G. Rajagopal, A. J. James, R. J. Needs, L. M. Fraser, W. M. C. Foulkes, and P. Maccullum, Phys. Rev. B **53**, 9640 (1996).
[5] H. Eckstein, W. Schattke, M. Reigrotzki, and R. Redmer, Phys. Rev. B **54**, 5512 (1996).
[6] A. Malatesta, S. Fahy, and G. B. Bachelet, Phys. Rev. B **56**, 12201 (1997).
[7] L. Mitáš and R. M. Martin, Phys. Rev. Lett. **72**, 2438 (1994).
[8] P. R. C. Kent, R. Q. Hood, M. D. Towler, R. J. Needs, and G. Rajagopal, Phys. Rev. B **57**, 15293 (1998).
[9] P. R. C. Kent, R. Q. Hood, A. J. Williamson, R. J. Needs, W. M. C. Foulkes, and G. Rajagopal, Phys. Rev. B **59**, 1917 (1999).
[10] W. M. C. Foulkes, L. Mitáš, R. J. Needs, and G. Rajagopal, Rev. Mod. Phys. **73**, 33 (2001).
[11] L. Hedin and S. Lundquist, Solid State Phys. **23**, 1 (1969).
[12] M. S. Hybertsen and S. G. Louie, Phys. Rev. B **34**, 5390 (1986).
[13] N. Metropolis, A. W. Rosenbluth, M. N. Rosenbluth, A. H. Teller, and E. Teller, J. Chem. Phys. **21**, 1087 (1953).
[14] D. Lukas, Ph.D. thesis, Kiel, 1996.
[15] T. Kato, Commun. Pure Appl. Math. **10**, 151 (1957).
[16] D. R. Hamann, M. Schlüter, and C. Chiang, Phys. Rev. Lett. **43**, 1494 (1979).
[17] D. R. Hamann, Phys. Rev. B **40**, 2980 (1989).
[18] The QIRM — Quantum Monte Carlo for Inhomogeneous Real Materials — package is publicly available at http://www.tp.cau.de/schattke/qirm/ or via email to qirm@tp.cau.de
[19] A. J. Williamson, G. Rajagopal, R. J. Needs, L. M. Fraser, W. M. C. Foulkes, Y. Wang, and M. Y. Chou, Phys. Rev. B **55**, R4851 (1997).